The Astrophysical Journal Supplement Series, 166:498–504, 2006 October

AN ATLAS OF *HUBBLE SPACE TELESCOPE* STIS SPECTRA OF SEYFERT GALAXIES[1]

P. F. Spinelli, T. Storchi-Bergmann, and C. H. Brandt
Instituto de Física, UFRGS, Porto Alegre, RS, Brazil; patricia.spinelli@ufrgs.br

and

D. Calzetti
Space Telescope Science Institute, Baltimore, MD 21218
Received 2005 November 7; accepted 2006 May 12

ABSTRACT

We present a compilation of spectra of 101 Seyfert galaxies obtained with the *Hubble Space Telescope* (*HST*) Space Telescope Imaging Spectrograph (STIS), covering the UV and/or optical spectral range. Information on all the available spectra have been collected in a Mastertable, which is a very useful tool for anyone interested in a quick glance at the existent STIS spectra for Seyfert galaxies in the *HST* archive, and it can be recovered electronically. Nuclear spectra of the galaxies have been extracted in windows of 0.″2 for an optimized sampling (as this is the slit width in most cases) and combined in order to improve the signal-to-noise ratio and provide the widest possible wavelength coverage. These combined spectra are also available electronically.

Subject headings: atlases — galaxies: nuclei — galaxies: Seyfert — ultraviolet: galaxies

Online material: machine-readable table

1. INTRODUCTION

Spectra obtained with the *HST* Space Telescope Imaging Spectrograph (STIS) provide unique information on the spectral energy distribution (SED) of active galactic nuclei (AGNs), in two aspects: the coverage of the ultraviolet spectral range, which is not observable from the ground, and the high angular resolution, which enhances the contrast between the nuclear continuum and that of the stars of the host galaxies. Now that STIS has ceased to work, it is timely to compile the data accumulated by observations with this instrument in an Atlas. In the present work we provide such a compilation for 101 Seyfert galaxies.

We have used the spectra to construct nuclear SEDs of Seyfert galaxies obtained from extractions at an optimized sampling, corresponding to an aperture 0.″2 × 0.″2, as 0.″2 is the width of the slit in most observations. These combined nuclear spectra are available electronically and can be used for a number of studies. The small extraction window allows us to better isolate the nuclear SED, minimizing the contamination by the bulge of the host galaxies. These spectra can be compared with data obtained through large apertures using ground-based telescopes in order to evaluate the contribution of the of host galaxies, particularly useful when studying samples of distant AGNs. These spectra can also be used to investigate the contribution of other sources very close to the nucleus, such as starbursts (Storchi-Bergmann et al. 2005; González Delgado et al. 2004).

Although the *HST* archive provides one-dimensional spectra, which are identified by the terminations `_x1d` and `_sx1`, our Atlas has at least three advantages:

1. The `_x1d` and `_sx1` spectra are obtained with a extraction window of 11 pixels for the UV corresponding to 0.″27, and 7 pixels for the optical—corresponding to 0.″35. Therefore, the extraction windows in the UV an optical are different and do not make optimal use the angular resolution provided by *HST*. Our extraction window is chosen to have the same angular extent of the slit width, 0.″2 in all wavelength ranges, providing spectra with better angular resolution. For AGNs, a smaller extraction window increases the contrast between the active nucleus and the host galaxy.
2. In many cases, the *HST* pipeline does not perform averages of spectra. This is the case of the `_x1d` spectra, which are very noisy.
3. The pipeline also does not "glue" the different spectral segments together. In the Atlas we have done this after eliminating the noisy borders of each spectral segment.

Our Atlas thus provides better signal-to-noise ratio nuclear spectra with the widest available spectral coverage, with the different spectral ranges already combined and edited to eliminate the noise usually present at the initial and final wavelengths of each segment.

In the process of constructing the Atlas, we have compiled relevant information on all the available spectra we have been collected in a Mastertable. It contains, for example, initial and final wavelengths of the different spectra segments, exposure times, gratings, and slit widths. This Mastertable is by itself a very useful tool for anyone interested in a quick glance at the available STIS spectra for Seyfert galaxies in the *HST* archive and can be recovered electronically as the spectra.

This paper is organized as follows: § 2 describes our sample selection. Section 3 presents the Mastertable and describes the information contained in it. The extraction of the spectra is described in § 4, and their combination is explained in § 5. The results and some potential applications are discussed in § 6.

2. SAMPLE AND DATA

The sample was initially selected as all Seyfert galaxies listed in the catalog of Véron-Cetty & Véron (1996) with redshift $z \leq 0.03$, which had STIS spectra available in the archive. We have

---

[1] Based on observations made with the NASA/ESA *Hubble Space Telescope*, obtained from the data archive at the Space Telescope Science Institute. STScI is operated by the Association of Universities for Research in Astronomy, Inc., under NASA contract NAS 5-26555.

TABLE 1

GALAXY SAMPLE

Galaxy	R.A. (J2000.0)[a]	Decl. (J2000.0)[a]	Hubble Type[a]	Activity[a]	Z[a]	Coverage (Å)	References
Q0038+327[b]	00 40 43.5	+32 58 33	. . .	Sy?	0.1970	1640–3175[b]	. . .
Mrk 348	00 48 47.1	+31 57 25	. . .	H II/WR, Sbrst, Sy2	0.1177	2500–5700	. . .
IRAS 01003−2238	01 02 49.9	−22 21 56	SB(rs)bc	Sy	0.0049	1140–10226	1
NGC 613	01 34 18.2	−29 25 07	SA(s)0/a	Sy2	0.0150	6482–7054	2, 3
Mrk 573	01 43 57.8	+02 21 00	(R)SAB(rs)0+	Sy2	0.0172	2900–6867	4
UM 146	01 55 22.0	+06 36 43	SA(rs)b	Sy1.9	0.0174	2900–6867	4
NGC 788	02 01 06.4	−06 48 56	SA(s)0/a	Sy1, Sy2	0.0136	2900–6867	4
3C 67	02 24 12.3	+27 50 12	. . .	BLRG	0.3102	2900–10226	5
NGC 985	02 34 37.8	−08 47 15	SBbc?p(Ring)	Sy1	0.0431	1194–1250	6
NGC 1052	02 41 04.8	−08 15 21	E4	LINER, Sy2	0.0049	6295–6867	7, 8
NGC 1068	02 42 40.7	−00 00 48	(R)SA(rs)b	Sy1, Sy2	0.0038	1140–10266	9, 10
NGC 1097[d]	02 46 19.0	−30 16 30	(R′_1:)SB(r′l)b	Sy1	0.0042	1140–10266[d]	. . .
Mrk 1066	02 59 58.6	+36 49 14	(R)SB(s)0+	Sy2	0.0120	2900–5700	. . .
NGC 1358	03 33 39.7	−05 05 22	SAB(r)0/a	Sy2	0.0134	2900–6867	4
MS 0335.4−2618[b]	03 37 36.6	−26 09 08	. . .	Sy1	0.1230	1150–1740[b]	. . .
3C 109	04 13 40.4	+11 12 14	Opt.var	Ngal, Sy1.8	0.3056	2900–10266	. . .
3C 120	04 33 11.1	+05 21 16	S0, LPQ	BLRG, Sy1	0.0330	2900–10266	. . .
Mrk 618[b]	04 36 22.2	−10 22 34	SB(s)b pec	Sy1	0.0355	1640–3175[b]	11
NGC 1667	04 48 37.1	−06 19 12	SAB(r)c	Sy2	0.0152	2900–6867	4
3C 135	05 14 08.3	+00 56 32	E	BLRG, Sy2	0.1274	5236–10266	12
AKN 120[b]	05 16 11.4	−00 08 59	Sb/pec	Sy1	0.0323	1640–3175[b]	11
IRAS 05189−2524	05 21 01.3	−25 21 45	pec	Sy2	0.0426	1140–10266	1
NGC 1961	05 42 04.8	+69 22 43	SAB(rs)c	LINER	0.0131	6295–6867	. . .
NGC 2110	05 52 11.4	−07 27 22	SAB0−	Sy2	0.0078	6295–6867	13
Mrk 3	06 15 36.3	+71 02 15	S0	Sy2	0.0135	1140–10266	14, 15
NGC 2273	06 50 08.7	+60 50 45	SB(r)a	Sy2	0.0062	2900–6867	4
Mrk 9[b]	07 36 57.0	+58 46 13	S0 pec?	Sy1.5	0.0399	1640–3175[b]	11
Mrk 78[b]	07 42 41.7	+65 10 37	SB	Sy2	0.0371	1140–7054[b]	16
NGC 2787	09 19 18.5	+69 12 12	SB(r)0+	LINER	0.0023	2900–6867	17, 18, 19, 20
NGC 2841	09 22 02.6	+50 58 35	SA(r)b	LINER, Sy1	0.0021	8275–8847	. . .
Mrk 110	09 25 12.9	+52 17 11	Pair?	Sy1	0.033	1194–1250	. . .
NGC 2911	09 33 46.1	+10 09 09	SA(s)0:pec	LINER, Sy	0.0106	6482–7054	. . .
NGC 3031	09 55 33.2	+69 03 55	SA(s)ab	LINER, Sy1.8	−0.0001	8275–8847/6265–6867	21, 22
NGC 3081	09 59 29.5	−22 49 35	(R_1)SAB(r)0/a	Sy2	0.0079	2900–6867	4
Mrk 34	10 34 08.6	+60 01 52	Spiral	Sy2	0.0505	2900–5700	. . .
NGC 3227	10 23 30.6	+19 51 54	SAB(s)pec	Sy1.5	0.0039	1140–10266	7, 8, 23
NGC 3393[d]	10 48 23.4	−25 09 43	(R′)SB(s)ab	Sy2	0.0125	2900–6867[d]	24
NGC 3516	11 06 47.5	+72 34 07	(R)SB(s)00	Sy1.5	0.0088	1140–5700/6265–6867	24, 25
IRAS 11058−1131	11 08 20.3	−11 48 12	. . .	Sy2	0.0548	2900–6867	24
ESO 438−G009[d]	11 10 48.0	−28 30 04	(R′_1)SB(rl)ab	Sy1.5	0.0234	1194–1250[d]	26
MCG 10.16.111	11 18 57.7	+58 03 24	. . .	Sy1	0.0279	1194–1250	26
NGC 3627	11 20 15.0	+12 59 30	SAB(s)b	LINER, Sy2	0.0024	2900–6867	. . .
SBS 1127+575[b]	11 30 03.6	+57 18 29	. . .	Sy2	0.0361	1194–1250[b]	26
PG 1149−110	11 52 03.5	−11 22 24	. . .	Sy1	0.0490	1194–1250	26
NGC 3982	11 56 28.1	+55 07 31	SAB(r)b	Sy2	0.0037	2900–6867	17, 18, 19, 20
NGC 3998	11 57 56.1	+55 27 13	SA(r)00?	LINER, Sy1	0.0035	8275–8847	. . .
NGC 4036	12 01 26.9	+61 53 44	S0−	LINER	0.0048	6295–6867	7, 8
3C 268.3	12 06 24.7	+64 13 37	. . .	BLRG	0.3710	5236–10266	12
NGC 4138	12 09 29.6	+43 41 17	SA(r)0+	Sy1.9	0.0030	2900–6867	17, 18, 19, 20
IRAS 12071−0444	12 09 45.1	−05 01 14	. . .	Sy2	0.1283	5236–10266	1
NGC 4151[d]	12 10 32.6	+39 24 21	(R′)SAB(rs)ab	Sy1.5	0.0033	1140–10266[d]	27–33
Mrk 766	12 18 26.5	+29 48 46	(R′)SB(s)a	Sy1.5	0.0129	1140–3184	. . .
NGC 4258[d]	12 18 57.5	+47 18 14	SAB(s)bc	LINER, Sy1.9	0.0015	8275–8847[d]	2, 3
NGC 4278	12 20 06.8	+29 16 51	E1–2	LINER, Sy1	0.0022	8275–8847	. . .
Q1219+047[b]	12 21 37.9	+04 30 26	. . .	Sy1	0.0940	1194–1250[b]	. . .
NGC 4303	12 21 54.9	+04 28 25	SAB(rs)bc	H II Sy2	0.0052	1568–10266	2, 3, 34
NGC 4450	12 28 29.6	+17 05 06	SA(s)ab	LINER, Sy3	0.0065	2900–10266	17, 18, 19, 20
NGC 4477	12 30 02.2	+13 38 11	SB(s)0?	Sy2	0.0045	2900–6867	17, 18, 19, 20
M87	12 30 49.4	+12 23 28	E+0–1pec	NLRG, Sy	0.0044	1140–10266	35
NGC 4501	12 31 59.2	+14 25 14	SA(rs)b	Sy2	0.0076	2900–6867	17, 18, 19, 20
Ton 1542	12 32 03.6	+20 09 29	Spiral	Sy1	0.0630	1194–1300	6
NGC 4540[b]	12 34 50.8	+15 33 05	SAB(rs)cd	LINER, Sy1	0.0043	2900–5700[b]	. . .
NGC 4507	12 35 36.6	−39 54 33	SAB(s)ab	Sy2	0.0118	2900–6867	4
NGC 4569	12 36 49.8	+13 09 46	SAB(rs)ab	LINER, Sy	−0.0008	2900–6867	. . .

TABLE 1—*Continued*

Galaxy	R.A. (J2000.0)[a]	Decl. (J2000.0)[a]	Hubble Type[a]	Activity[a]	Z[a]	Coverage (Å)	References
NGC 4579	12 37 43.6	+11 49 05	SAB(rs)b	LINER, Sy1.9	0.0051	6295–6867	7, 8
NGC 4594	12 39 59.4	−11 37 23	SA(s)a	LINER, Sy1	0.0034	6482–7054	. . .
IC 3639	12 40 52.8	−36 45 21	SB(rs)bc	Sy2	0.0109	2900–6867	4
NGC 4698	12 48 22.9	+08 29 14	SA(s)ab	Sy2	0.0033	2900–6867	17, 18, 19, 20
NGC 4736	12 50 53.0	+41 07 14	(R)SA(r)ab	LINER, Sy2	0.0010	6295–6867	. . .
NGC 4826	12 56 43.7	+21 40 52	(R)SA(rs)ab	Sy2	0.0014	2900–6867	. . .
NGC 5005	13 10 56.2	+37 03 33	SAB(rs)bc	Sy2, LINER	0.0032	6482–7054	2, 3
IRAS 13224−3809[d]	13 25 19.3	−38 24 53	. . .	Sbrst, NLSy1	0.0667	5236–10266[d]	36, 37
NGC 5135	13 25 44.0	−29 50 01	SB(l)ab	Sy2	0.0137	2900–5700/6295–6768	4
NGC 5194[c]	13 29 52.7	+47 11 43	SA(s)bc pec	H II Sy2.5	0.0015	2900–10266[c]	38
NGC 5252	13 38 15.9	+04 32 33	S0	Sy1.9	0.0230	2900–5700	24
NGC 5283	13 41 05.7	+67 40 20	S0?	Sy2	0.0104	2900–6867	4
Ton 730	13 43 56.7	+25 38 48	. . .	Sy1	0.0870	1194–1250	26
NGC 5347	13 53 17.8	+33 29 27	(R′)SB(rs)ab	Sy2	0.0078	2900–6867	4
Mrk 463E	13 56 02.9	+18 22 19	. . .	Sy1, Sy2	0.0500	2900–5700	. . .
NGC 5427	14 03 26.0	−06 01 51	SA(s)c, pec	Sy2	0.0087	2900–6867	4
Circinus	14 13 09.9	−65 20 21	SA(s)b	Sy2	0.0014	4818–5104	. . .
NGC 5635	14 28 31.7	+27 24 32	S, pec	LINER, Sy3	0.0144	6482–7054	. . .
NGC 5643	14 32 40.8	−44 10 29	SAB(rs)c	Sy2	0.0040	2900–6867	4
Mrk 817[b]	14 36 22.1	+58 47 39	SBc	Sy1.5	0.0314	2758–2914[b]	39
NGC 5695	14 37 22.1	+36 34 04	SBb	Sy2	0.0141	2900–6867	4
NGC 5728	14 42 23.9	−17 15 11	(R_1)SAB(r)a	Sy2	0.0093	6295–6867	. . .
IRAS 15206+3342[b]	15 22 38.0	+33 31 36	?	H II Sy2	0.1244	1140–10266[b]	1
3C 346	16 43 48.6	+17 15 49	E	NLRG, Sy2	0.1620	2900–10266	12
1701+610	17 02 11.1	+60 58 48	. . .	Sy1.9	0.1649	1140–10266	. . .
NGC 6300	17 16 59.5	−62 49 14	SB(rs)b	Sy2	0.0037	6581–6867	4
PKS 1739+184[d]	17 42 06.9	+18 27 21	. . .	Sy1	0.1860	1140–5700[d]	. . .
3C 405[b]	19 59 28.3	+40 44 02	S?	Radiogal, Sy2	0.0561	2900–5700[b]	40, 41
3C 382	18 35 02.1	+32 41 50	. . .	BLRG, Sy1	0.0579	2900–10266	. . .
3C 390	18 45 37.6	+09 53 45	. . .	RadioS	. . .	2900–5700	. . .
NGC 6951	20 37 14.1	+66 06 20	E+pec?	. . .	0.0129	6482–7054	2, 3
3C 445	22 23 49.6	−02 06 12	N galaxy	BLRG, Sy1	0.0562	2900–10266	. . .
NGC 7314	22 35 46.2	−26 03 01	SAB(rs)bc	Sy1.9	0.0048	2900–10266	2, 3
AKN 564[d]	22 42 39.3	+29 43 31	SB	Sy1.8	0.0247	1140–3184[d]	43, 44, 45
IC 1459	22 57 10.6	−36 27 44	E3	LINER	0.0056	2900–5700	42
NGC 7674	23 27 56.7	+08 46 45	SA(r)bc pec	H II Sy2	0.0289	2900–5700	. . .
NGC 7682	23 29 03.9	+03 32 00	SA(r)bc pec	H II Sy2	0.0289	2900–6867	4

NOTE.—Units of right ascension are hours, minutes, and seconds, and units of declination are degrees, arcminutes, and arcseconds.

[a] References from NASA/IPAC Extragalactic Database.

[b] Spectra of this galaxy were not extracted due to a poor signal-to-noise ratio in the continuum. Nevertheless, information on the available spectra is also included in the Mastertable.

[c] Spectra of this galaxy were not extracted due to the presence of more than one continuum source where we could not identify the brightest one. Information on the available spectra is also included in the Mastertable.

[d] Final spectrum of this Seyfert 1 galaxy was obtained with spectra observed in different dates.

REFERENCES.—(1) Farrah et al. 2005; (2) Hughes et al. 2003; (3) Hughes et al. 2005; (4) Pogge et al. 2003; (5) O'dea et al. 2003 ; (6) Penton et al. 2004; (7) Barth et al. 2001a; (8) Barth et al. 2001b; (9) Kraemer et al. 2000b ; (10) Cecil et al. 2002; (11) Jenkins et al. 2003; (12) Hutchings et al. 1998; (13) Ferruit et al. 2004; (14) Collins et al. 2005 ; (15) Ruiz et al. 2001; (16) Whittle et al. 2005; (17) Sarzi et al. 2001; (18) Sarzi et al. 2002; (19) Sarzi et al. 2005; (20) Ho et al. 2002; (21) Chandar et al. 2001a; (22) Chandar et al. 2001b; (23) Crenshaw et al. 2001; (24) Cappetti et al. 2005; (25) Edelson et al. 2000; (26) Bowen 2002; (27) Kaiser et al. 2000; (28) Kraemer et al. 2000a; (29) Nelson 2000; (30) Hutchings et al. 1999; (31) Crenshaw et al. 2000; (32) Hutchings et al. 2002; (33) Kraemer et al. 2001 ; (34) Colina et al. 2002; (35) Sabra et al. 2003; (36) Leighly 2004 ; (37) Leighly & Moore 2004; (38) Bradley et al. 2004; (39) Jenkins et al. 2003; (40) Tadhunter et al. 2003; (41) Bellamy & Tadhunter 2004; (42) Cappellari et al. 2002; (43) Crenshaw et al. 2002 ; (44) Collier et al. 2001; (45) Romano et al. 2004.

later tried to incorporate the remaining Seyfert galaxies ($z \geq 0.03$). Misclassification, however, may have prevented a comprehensive inclusion of all Seyfert galaxies in the *HST* archive. Thus, our sample comprises most galaxies (101 in the total) classified as Seyfert with available STIS spectra in the *HST* archive until 2004 September. Although the most valuable wavelength range is the UV because it is not accessible from the ground, we have included in the Atlas also those cases in which only optical spectra were available. The sample galaxies are listed in Table 1, which contains information on the positions, Hubble type, activity type, redshift, and references to previous works in which the spectra have been used. The seventh column of Table 1 gives the spectral coverage (in the observed frame) of the resulting nuclear spectrum after the individual extractions and combination of the different spectral segments.

3. THE MASTERTABLE

Relevant information about all the two-dimensional (2D) spectra collected is summarized in a Mastertable, available electronically.[2] The columns of the table contain the following information: (1) the name of the galaxy; (2) the identification of all available STIS spectra for this galaxy in the *HST* archive, one per

---

[2] See www.if.ufrgs.br/~pat/atlas.htm.

TABLE 2

A Sample of Lines from the Mastertable

Galaxy (1)	Root Name (2)	Grating (3)	Aperture (arcsec^2) (4)	λ_c (Å) (5)	λ_i (Å) (6)	λ_f (Å) (7)	R (8)	P.A. (deg) (9)	Exposure Time (s) (10)	Name (11)	Scale (arcsec pixel^{-1}) (12)
MCG 10.16.111	o5ew02010	G140M	52 × 0.2	1222	1194	1250	12200	−86.5063	3900	m1016111-1.234	0.029
	o5ew02020	G140M	52 × 0.2	1222	1194	1250	12200	−86.5063	3900	m1016111-2.234	0.029
	o5ew02030	G140M	52 × 0.2	1222	1194	1250	12200	−86.5063	3900	m1016111-3.234	0.029
	o5ew02040	G140M	52 × 0.2	1222	1194	1250	12200	−86.5063	3900	m1016111-4.234	0.029
	o5ew02050	G140M	52 × 0.2	1222	1194	1250	12200	−86.5062	3900	m1016111-5.234	0.029
NGC 3627......................	o63n02010	G430L	52 × 0.2	4300	2900	5700	800	80.0559	2349	n3627-1.80	0.1
	o63n02020	G750M	52 × 0.2	6581	6295	6867	5980	80.0559	2861	n3627-2.80	0.1
PG 1149−110	o5ew05010	G140M	52 × 0.2	1222	1194	1250	12200	43.6861	2269	p1149-1.44	0.029
	o5ew05020	G140M	52 × 0.2	1222	1194	1250	12200	43.6861	2899	p1149-2.44	0.029
	o5ew05030	G140M	52 × 0.2	1222	1194	1250	12200	43.6861	2899	p1149-3.44	0.029
NGC 3982......................	o4e006010	G750M	52 × 0.2	6581	6295	6867	5980	117.931	900	n3982-1.117	0.05
	o4e006020	G750M	52 × 0.2	6581	6295	6867	5980	117.931	1197	n3982-2.117	0.05
	o4e006030	G750M	52 × 0.2	6581	6295	6867	5980	117.931	900	n3982-3.117	0.05
	o4e006040	G430L	52 × 0.2	4300	2900	5700	800	117.931	900	n3982-4.117	0.05
	o4e006050	G430L	52 × 0.2	4300	2900	5700	800	117.931	945	n3982-5.117	0.05
IRAS 15206+3342.........	o5f904030	G430L	52 × 0.2	4300	2900	5700	800	35.3559	780	i1520-3.35	0.05
	o5f904040	G430L	52 × 0.2	4300	2900	5700	800	35.3559	650	i1520-4.35	0.05
	o5f904050	G750L	52 × 0.2	7751	5236	10266	790	35.356	624	i1520-5.35	0.05
	o5f904060	G750L	52 × 0.2	7751	5236	10266	790	35.3559	624	i1520-6.35	0.05
	o5f904070	G750L	52 × 0.2	7751	5236	10266	790	35.3559	545	i1520-7.35	0.05
	o5f904090	G140L	52 × 0.2	1425	1140	1730	1190	35.3001	900	i1520-8.35	0.0244

Notes.—Columns: (1) Name of the galaxy; (2) identification of all available STIS spectra for this galaxy in the *HST* archive, one per line; (3) grating used in each observation; (4) slit width of each observation; (5) central wavelength; (6) initial wavelength; (7) final wavelength; (8) spectral resolution; (9) slit orientation; (10) exposure time; (11) identification of the extracted spectrum from each segment; (12) plate scale of the observations. Table 2 is available in its entirety in the electronic edition of the *Astrophysical Journal Supplement*. A portion is shown here for guidance regarding its form and content.

line; (3) the grating used in each observation; (4) the slit width of each observation; (5) the central wavelength (in the observed frame); (6) the initial wavelength (in the observed frame); (7) the final wavelength (in the observed frame); (8) the spectral resolution; (9) the slit orientation; (10) the exposure time. In column (11) we list the identification of the extracted spectrum from each segment, which will be useful in a few cases where we could not combine the spectra of the same galaxy (e.g., because they were obtained in different slit positions) and we then provide the individual extracted spectra without combining them. These spectra are identified according to following convention: compact name of the galaxy followed by an arbitrary ordering number and the slit orientation. For example, n3516-13.97 means the 13th spectrum of the galaxy NGC 3516, which was obtained at slit orientation of 97°. Finally, in column (12) we list the plate scale of the observations. In Table 2 we present a printout of a few selected lines of the Mastertable (which has 1001 lines), for illustrative purposes.

4. EXTRACTION OF THE SPECTRA

The nuclear spectra were obtained from 2D reduced STIS spectra, which have been rectified and wavelength and flux calibrated, and are identified in the *HST* archive by the suffixes `_x2d` and `_sx2`. The latter are summed `_x2d` spectra (when the observations were performed in the `cr-split` or `repeatobs` modes). When both `_x2d` and `_sx2` spectra were available, we used the latter.

One-dimensional (1D) spectra were extracted from the 2D spectra in windows of 0″.2 from a long-slit spectrum usually obtained through a slit width 0″.2 and covering 52″ in the sky. The IRAF task `apall` was used to perform the extractions. We performed the sky subtraction by fitting a straight line to regions along the slit with no (or negligible) galaxy contribution. For each galaxy, different sky windows were defined, in order to avoid including contribution from the galaxy. The sky level was always negligible, except in the Lyα Geocoronal emission line.

Although the redshift range for the sample is $0 \leq z \leq 0.37$, only for 15% of the galaxies with $z \geq 0.06$, such that the 0″.2 aperture corresponds at the galaxies to more than 200 pc. For 60% of the sample, 0″.2 corresponds to <60 pc at the galaxies, while for 30% of the sample it corresponds to <20 pc. We are thus sampling a very small region around the active nucleus, providing the best possible contrast between the AGN and galaxy bulge.

We extracted only nuclear spectra that we identified as being centered at the peak of the continuum flux along the slit. This was done by inspecting the spatial light distribution in a spectral region devoid of emission or strong absorption lines (the continuum) and centering the extraction window at the peak of the continuum flux distribution. In a few cases, the 2D spectra contained only emission lines, with no continuum. In these cases, for which we could not identify a continuum source, we did not extract the spectra, but the information on the available 2D spectra are still listed in the Mastertable, with a cautionary note explaining why the spectra have not been extracted.

In the cases for which there were more than one continuum source we extracted the brightest one. Although we cannot be absolutely sure for all cases, Seyfert galaxies are usually the brightest object. There are two exceptions, for which we did not extract the spectra because the two sources were equally bright. These two cases have also been identified in the Mastertable with a cautionary note.

After extracting the spectra, for the galaxies that had more than one exposure for each spectral range (and with the same spectral resolution, orientation and plate scale), we constructed averages to improve the signal-to-noise ratio, eliminating also

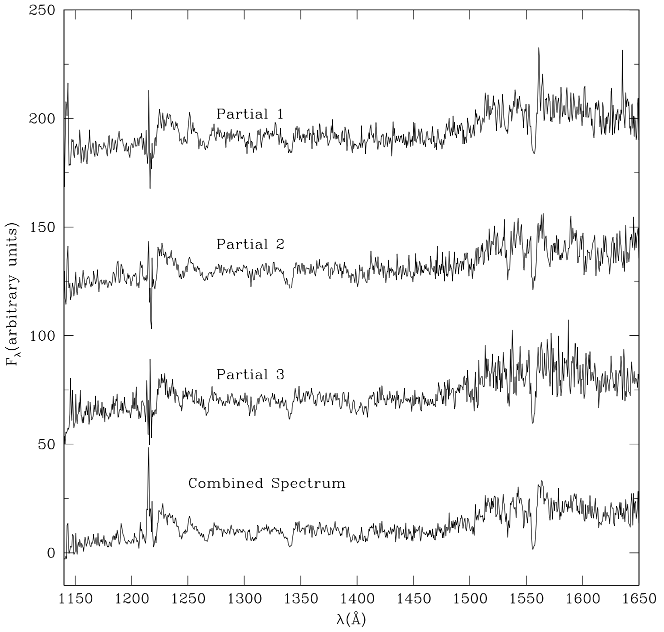

FIG. 1.—Illustration of the process of averaging three UV spectra (observed frame) of the galaxy NGC 1097.

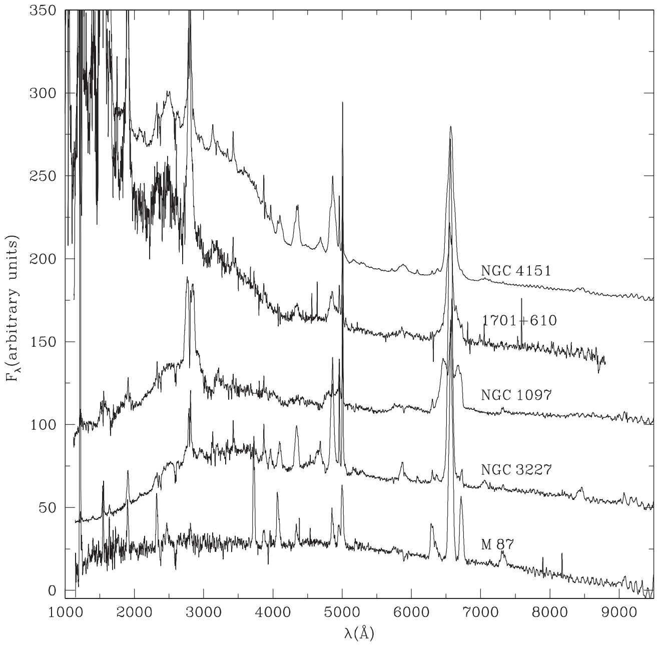

FIG. 3.—Illustration of 5 of the 9 spectra with widest spectral coverage. The spectra have been shifted to the rest frame of the galaxies.

cosmic rays and other defects when detected. The average was only constructed after checking also if the spectra had similar flux level. For the construction of the average spectra we have used the task `scombine` in IRAF, with the rejection algorithm `avsigclip` when three or more spectra were available or `minmax` when there were only two spectra. This step is illustrated in Figure 1.

5. COMBINATION OF THE SPECTRA

The final spectra were obtained by combining the data from the different spectral ranges using the same task `scombine` in IRAF, after editing out noisy regions at the borders of each spectral segment and checking that there were no significant differences between their fluxes. We did not find such differences for most of the cases in which there was a significant superposition of adjacent spectral segments. This final step is illustrated in Figure 2.

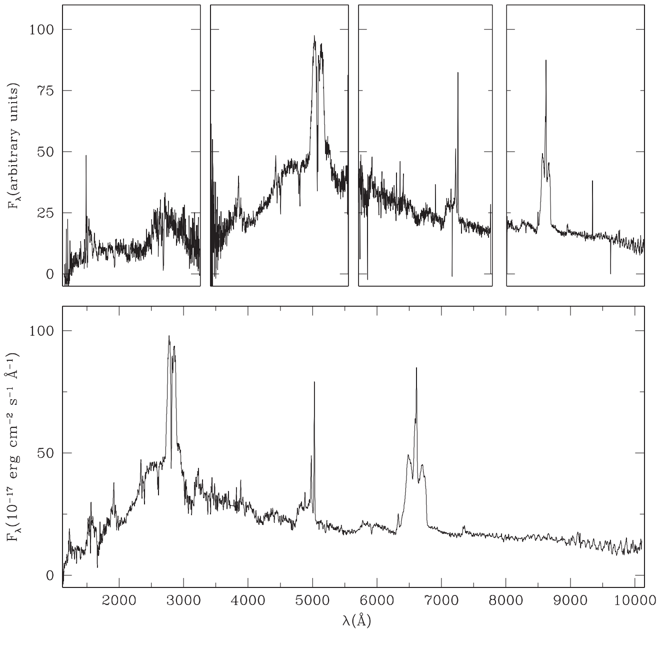

FIG. 2.—Illustration of the process of combining different spectral segments (observed frames) for the galaxy NGC 1097.

In the case of the Seyfert 1 galaxies there is the issue of variability, so that spectra obtained in different dates may show different fluxes, in line and continua. We have checked the dates and found only five cases of Seyfert 1 galaxies with spectral segments obtained in different dates: NGC 4151, NGC 4258, PKS 1739+184, and AKN 564. In the case of IRAS 13224−3809, 2 of the combined 7 spectra were obtained one day latter than the other 5, thus the effect of variability should be minimal. We have identified these cases with a note in Table 1 and in the Mastertable. Nevertheless, we did not find any obvious discrepancy in fluxes when combining the different spectral segments of these galaxies.

Finally, we would like to point out that, prior to the extraction, the flux units were ergs s^{-1} cm^{-2} Å^{-1} arcsec^{-2} (see STIS Data Handbook). When we performed the extraction with `apall` to sum over a few pixels ($0\farcs2$ aperture) along the slit direction, the extracted spectrum is in units equivalent to pixel ergs s^{-1} cm^{-2} Å^{-1} arcsec^{-2}. Then, in order to consistently provide the flux integrated in the extraction window, in units of ergs s^{-1} cm^{-2} Å^{-1}, we multiplied each segment by a factor that is the product of the slit width and plate scale. For example, for one segment with a slit width of $0\farcs2$ and plate scale $0\farcs024$ pixel^{-1}, the factor is 0.0048 arcsec^{-2} pixel^{-1}. For another segment with plate scale $0\farcs05$ pixel^{-1}, with the same slit width, the factor is 0.01 arcsec^{-2} pixel^{-1}.

6. RESULTS

The combined spectra presenting the largest spectral coverage are shown in Figures 3 and 4. There are only 9 galaxies for which we could obtain the complete STIS UV-optical spectral coverage (∼1000–10000 Å).

In Figures 5, 6, and 7 we show the redshift corrected spectra for the galaxies with UV coverage in the 1100–1600 Å wavelength range, useful for looking for signatures of starbursts. In order to do that, we have drawn in the figures vertical lines at the locations of the absorption features characteristic of starbursts.

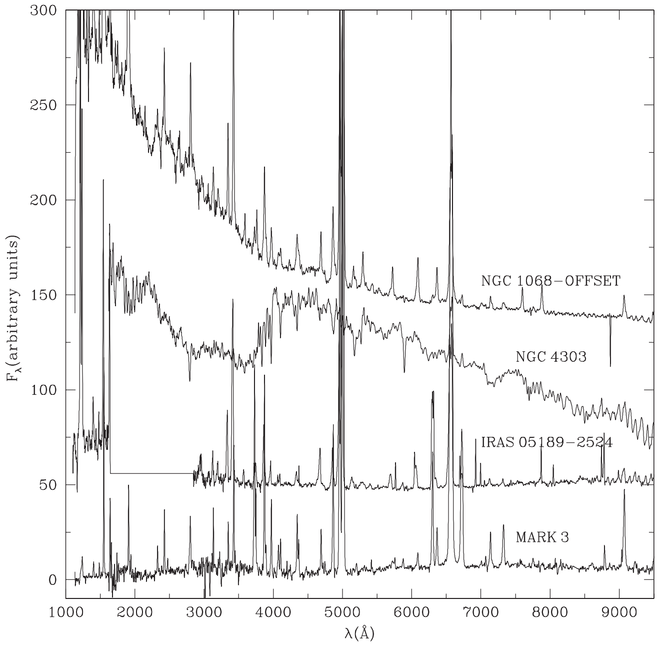

FIG. 4.—Same as Fig. 3 for another four spectra.

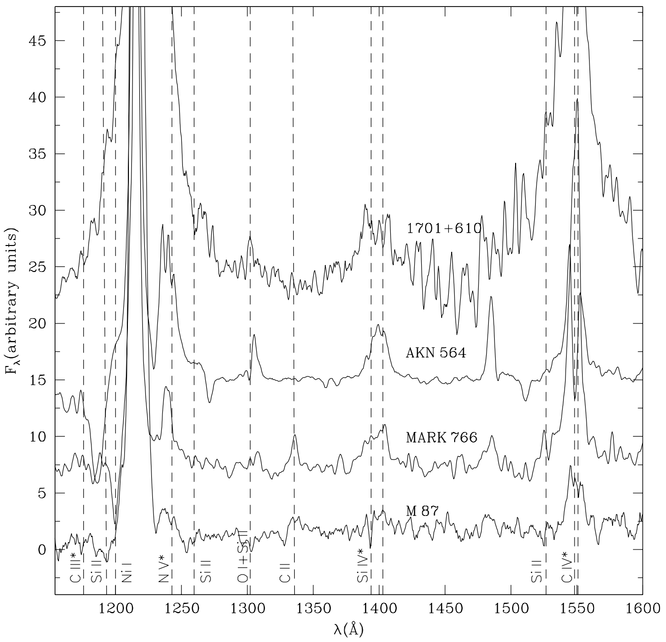

FIG. 6.—Same as Fig. 5 for another four spectra.

While most lines are interstellar, we identify by asterisks (*) the ones that originate in the atmosphere of young stars (Kinney et al. 1993; Vazquez et al. 2004), which are C III λ1175.65, N V λλ1238.81, 1242.80, C II λλ1334.53, 1335.70, Si IV λλ1393.76, 1402.77, and C IV λλ1548.20, 1550.77. Both the interstellar and stellar features of a starburst have been found in the UV spectrum of NGC 1097, as pointed out by Storchi-Bergmann et al. (2005). Figure 5 shows that the same features seem to be present in the spectrum of NGC 3227, suggesting that, also in this case, as in NGC 1097, there is a starburst closer than 8 pc from the nucleus in NGC 3227 (the distance at the galaxy corresponding to 0″.1 the angular distance from the nucleus covered by the aperture of the nuclear extraction). Indeed, the presence of traces of young stellar population in an optical nuclear spectrum of NGC 3227 have been previously reported by González Delgado & Perez (1997). These features seem also to be present in the spectrum of NGC 4151, but this has to be investigated further, as they may be due to absorptions in our galaxy, due to the proximity of NGC 4151. An obvious case of interstellar absorptions from our galaxy can be observed in the UV spectrum of NGC 3516 (Fig. 5), where absorptions from O I λ1302.08 + Si II λ1304.40 and C II λλ1334.53, 1335.70 originating in the Milky Way appear blueshifted from their wavelengths due to the shift of the spectrum to the rest frame of the galaxy.

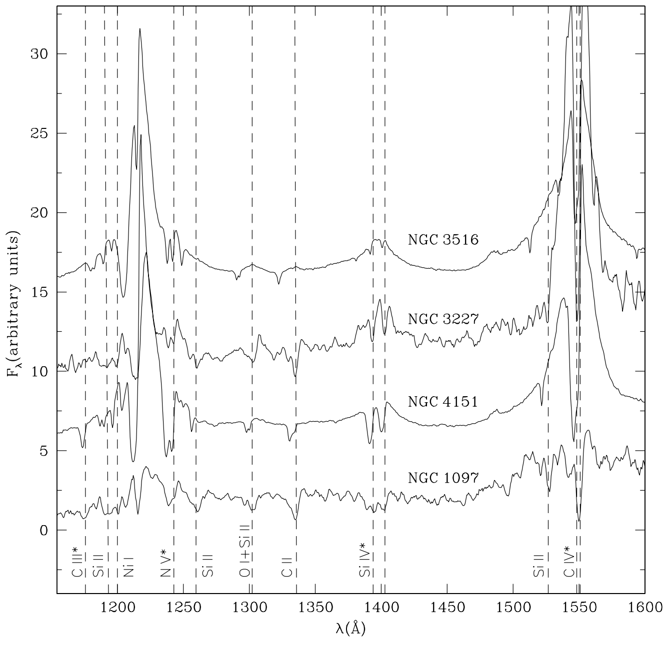

FIG. 5.—Illustration of 4 of the 12 spectra with UV coverage in the 1100–1600 Å wavelength range. The spectra have been shifted to the rest frame of the galaxies. The vertical dashed lines show the location of absorption features typical of starbursts. Asterisks (*) identify the absorption lines that originate in the atmosphere of early-type stars.

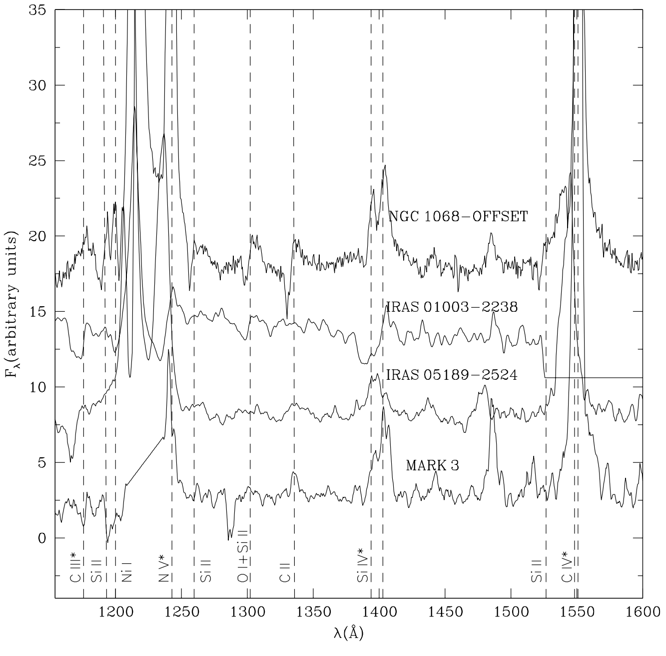

FIG. 7.—Same as Fig. 5 for another four spectra.

All spectra are available electronically (see footnote 2), where they can be visualized and recovered by clicking on the name of the galaxy. We also make available at the above address the Mastertable, which has a compilation of the relevant information on each spectrum used in the combination.

Finally, we point out that there are several spectra that were obtained only with the highest resolution gratings, therefore covering a short wavelength range. In many cases there is also a sequence of such spectra obtained at adjacent slit positions, apparently for kinematic studies. In these cases, we did not combine the spectra but provide instead the individual extractions in a tar file.

This work has been supported by the Brazilian agencies CNPq, CAPES, and FAPERGS. This research has made use of the NASA/IPAC Extragalactic Database (NED), which is operated by the Jet Propulsion Laboratory, Caltech, under contract with the National Aeronautics and Space Administration.

REFERENCES

Barth, A. J., et al. 2001a, ApJ, 555, 685
———. 2001b, ApJ, 546, 205
Bellamy, M. J., & Tadhunter, C. N. 2004, MNRAS, 353, 105
Bowen, D. V. 2002, ApJ, 580, 169
Bradley, L. D., Kaiser, M. E., & Baan, W. A. 2004, ApJ, 603, 463
Capetti, A., Marconi, A., Macchetto, D., & Axon, D. 2005, A&A, 431, 465
Cappellari, M., et al. 2002, ApJ, 578, 787
Cecil, G., et al. 2002, ApJ, 568, 627
Chandar, R., Ford, H. C., & Tsvetanov, Z. 2001a, AJ, 122, 1330
———. 2001b, AJ, 122, 1342
Colina, L., González Delgado, R., Mas-Hesse, J. M., & Leitherer, C. 2002, ApJ, 579, 545
Collier, S., et al. 2001, ApJ, 561, 146
Collins, N. R., et al. 2005, ApJ, 619, 116
Crenshaw, D. M., et al. 2000, ApJ, 545, L27
———. 2001, ApJ, 555, 633
———. 2002, ApJ, 566, 187
Edelson, R. 2000, ApJ, 534, 180
Farrah, D., et al. 2005, ApJ, 626, 70
Ferruit, P., et al. 2004, MNRAS, 352, 1180
González Delgado, R. M., & Perez, E. 1997, MNRAS, 284, 931
González Delgado, R., et al. 2004, ApJ, 605, 127
Ho, L. C., et al. 2002, PASP, 114, 137
Hughes, M. A., et al. 2003, AJ, 126, 742
———. 2005, AJ, 130, 73
Hutchings, J. B., et al. 1998, AJ, 116, 634
———. 1999, AJ, 118, 2101
———. 2002, AJ, 124, 2543
Jenkins, E. B., et al. 2003, AJ, 125, 2824
Kaiser, M. E., et al. 2000, ApJ, 528, 260
Kinney, A., Bohlin, R. C., Calzetti, D., Panagia, N., & Wuse, R. F. G. 1993, ApJS, 86, 5
Kraemer, S. B., et al. 2000a, ApJ, 531, 278
———. 2000b, ApJ, 544, 763
———. 2001, ApJ, 551, 671
Leighly, K. M. 2004, ApJ, 611, 125
Leighly, K. M., & Moore, J. R. 2004, ApJ, 611, 107
Nelson, C. H. 2000, ApJ, 531, 257
O'Dea, C., et al. 2003, Publ. Astron. Soc. Australia, 20, 88
Penton, S. V., Stocke, J. T., & Shull, J. M. 2004, ApJS, 152, 29
Pogge, R., Fields, D. L., Martini, P., & Shields, J. 2003, in ASP Conf. Ser. 290, Active Galactic Nuclei: from Central Engine to Host Galaxies, ed. S. Collin, F. Combes & I. Schlosman (San Francisco: ASP), 239
Romano, P., et al. 2004, ApJ, 602, 635
Ruiz, J. R., et al. 2001, AJ, 122, 2961
Sabra, B. M., et al. 2003, ApJ, 584, 164
Sarzi, M., et al. 2001, ApJ, 550, 65
———. 2002, ApJ, 567, 237
———. 2005, ApJ, 628, 169
Storchi-Bergmann, T., et al. 2005, ApJ, 624, L13
Tadhunter, C., et al. 2003, MNRAS, 342, 861
Véron-Cetty, M. P., & Veron, P. 1996, A Catalogue of Quasars and Active Nuclei (7th ed.; Garching: ESO)
Vazquez, G. A., et al. 2004, ApJ, 600, 162
Whittle, M., Rosario, D. J., Silverman, J. D., Nelson, C. H., & Wilson, A. S. 2005, AJ, 129, 104